



# Absorption Line Oscillator Strengths for the $C^2\Pi(0)$ - $A^2\Sigma^+(0)$ Band of Nitric Oxide

A. M. Velasco and C. Lavín

Departamento de Química Física y Química Inorgánica, Facultad de Ciencias, Universidad de Valladolid, E-47005 Valladolid, Spain; [anamaria.velasco.sanz@uva.es](mailto:anamaria.velasco.sanz@uva.es)  
Received 2023 June 5; revised 2023 July 26; accepted 2023 July 28; published 2023 September 1

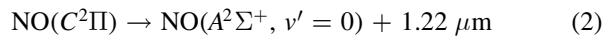
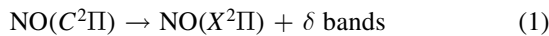
## Abstract

We have determined absorption oscillator strengths for rotational transitions of the  $C^2\Pi(0)$ - $A^2\Sigma^+(0)$  band of NO, which has been detected in the upper atmosphere of Venus. The molecular quantum defect orbital method has been used in the calculation of the electronic transition moment and the Rydberg-valence interaction between the  $C^2\Pi(v = 0)$  and the  $B^2\Pi(v = 7)$  states has been considered. Considerable deviations from normal intensity distribution of the rotational lines have been found at  $J \leq 5.5$ . As far as we know, the present line  $f$ -values are reported here for the first time. These data may be useful in the interpretation of the observations obtained by the Visible and Infrared Thermal Imaging Spectrometer instrument on the Venus Express spacecraft.

*Unified Astronomy Thesaurus concepts:* Molecular spectroscopy (2095); Line intensities (2084)

## 1. Introduction

Spectroscopy properties of the nitric oxide radical (NO) are of considerable astrophysical interest since NO has been detected in several interstellar environments including Sgr B2 (Liszt & Turner 1978), molecular clouds (McGonagle et al. 1990; Ziurys et al. 1991; Gerin et al. 1992), circumstellar envelopes (Quintana-Lacaci et al. 2013), and extragalactic sources (Martin et al. 2003). NO is also present in the upper atmospheres of Earth (Barth 1964), Venus (Feldman et al. 1979), and Mars (Bertaux et al. 2005). NO emissions are an important part of the upper atmospheric nightglow of all three planets. As described by Tennyson et al. (1986), the emission process is produced by radiative recombination of nitrogen and oxygen atoms giving NO molecules in the  $C^2\Pi$  Rydberg state. This state can decay radiatively through the following processes:



giving rise to band systems in different wavelength regions: both  $\delta$  ( $\text{C}^2\Pi$ - $\text{X}^2\Pi$ ) and  $\gamma$  ( $\text{A}^2\Sigma^+$ - $\text{X}^2\Pi$ ) band systems emit in the ultraviolet (UV) spectral region and the  $\text{C}^2\Pi$ - $\text{A}^2\Sigma^+$  transition, also known as the Heath band system, emits in the near-infrared (IR) region.

The presence of the  $\delta$  and  $\gamma$  bands of NO in the atmospheric nightglow of Earth, Venus, and Mars planets is well known. First observations of both bands in the UV nightglow of Earth were performed by Cohen-Sabban & Vuillemin (1973) using a balloon-borne spectrometer and by Feldman & Takacs (1974) with a rocket-borne spectrometer. The  $\delta$ -band system of NO in the UV nightglow of Venus was first identified by Feldman et al. (1979) using the International Ultraviolet Explorer. Stewart & Barth (1979), from spectra obtained with the Pioneer Venus Orbiter, pointed out that the nightglow spectrum of Venus in the UV is dominated by the  $v' = 0$  progressions of the

$\delta$  and  $\gamma$  bands of NO. Later, Bertaux et al. (2005) identified both band systems of nitric oxide in the Martian nightglow spectra obtained with the SPICAM UV spectrometer on board Mars Express. More recently, Muñoz et al. (2009) identified the  $\text{C}^2\Pi(0)$ - $\text{A}^2\Sigma^+(0)$  band, at  $1.224 \mu\text{m}$ , in the Venus nightglow spectra obtained by the Visible and Infrared Thermal Imaging Spectrometer (VIRTIS) instrument on the Venus Express spacecraft. These authors suggested that the  $\text{C}^2\Pi(0)$ - $\text{A}^2\Sigma^+(0)$  band should also be present along with the  $\text{C}^2\Pi(0)$ - $\text{X}^2\Pi(v'')$  and  $\text{A}^2\Sigma^+(0)$ - $\text{X}^2\Pi(v'')$  bands in the atmospheres of Earth and Mars. The interpretation of the observations of such atmospheres and, in particular, the planetary atmospheric modeling requires reliable spectroscopic data.

The  $\text{C}^2\Pi(0)$ - $\text{A}^2\Sigma^+(0)$  band of NO, which is the object of the present study, has been less investigated than the  $\delta$  and  $\gamma$  bands. Young & Sharpless (1962) observed a sharp line-like feature at  $1.223 \mu\text{m}$  in their infrared spectrograms and assigned it to the  $Q$  branches of the  $\text{C}^2\Pi$ - $\text{A}^2\Sigma^+$  transition. Later, Wray (1969) observed the shoulder R-branch of the  $\text{C}^2\Pi$ - $\text{A}^2\Sigma^+$  system in a study of the emissivity of air and nitrogen in the  $0.9$ - $1.2 \mu$  portion of the near-IR. The first description of the structure of  $\text{C}^2\Pi(0)$ - $\text{A}^2\Sigma^+(0)$  band was given by Ackerman & Miescher (1969) using a vacuum grating spectrometer but, as they indicated, the resolution obtained was unsatisfactory. The strong  $Q$  branch was also observed by Groth et al. (1971); Benesch & Saum (1972), and Lin (1974). Dingle et al. (1975) resolved the  $Q$  branch with a moderate resolution by using a SISAM interferometer. Amiot & Verges (1982) resolved the rotational structure of the  $\text{C}^2\Pi(0)$ - $\text{A}^2\Sigma^+(0)$  band by using a high-resolution Fourier Transformer Spectrometer and reported the wavenumbers of individual lines. Transition intensity data are particularly scarce for this band. Wray (1969) reported the absorption electronic oscillator strength for the  $\text{C}^2\Pi$ - $\text{A}^2\Sigma^+$ -band system from arc experiments. Groth et al. (1971) derived the oscillator strength for the  $\text{C}^2\Pi(0)$ - $\text{A}^2\Sigma^+(0)$  band from the intensities of the  $\delta$  and  $\gamma$  bands measured with a dry ice cooled PbS cell and Velasco et al. (2010) calculated it with the molecular quantum defect orbital (MQDO) method.

To the best of our knowledge,  $f$ -values for rotational transitions of the  $\text{C}^2\Pi(0)$ - $\text{A}^2\Sigma^+(0)$  band of NO have not yet been reported. Our specific interest in the rotational study of this band is motivated by both its presence in the nightglow of Venus and the scarcity of information available in the literature.



Original content from this work may be used under the terms of the [Creative Commons Attribution 4.0 licence](#). Any further distribution of this work must maintain attribution to the author(s) and the title of the work, journal citation and DOI.

In this work, we present transition energies and oscillator strengths, or  $f$ -values, of  $P$ ,  $Q$ , and  $R$  branches of the  $C^2\Pi(0)-A^2\Sigma^+(0)$  band of NO. It is known, that the  $C^2\Pi(0)$  Rydberg state is perturbed by the  $B^2\Pi(7)$  valence state (Lagerqvist & Miecher 1958; Galluser & Dressler 1982). The eigenvalues and eigenvectors of the perturbed states are obtained by diagonalization of a  $J$  dependent matrix in which the interaction parameters are obtained by fitting the eigenvalues to the observed energies. The MQDO method has been employed to calculate the electronic transition moment. Very recently, we obtained satisfactory results of rovibronic oscillator strengths for bands belonging to the  $\delta(C^2\Pi-X^2\Pi)$  system of NO by applying this procedure (Lavín & Velasco 2022).

## 2. Method of Calculation

The MQDO approach has been broadly used to determine one-photon transition intensities in molecules. A full description of this approach has been provided previously (Martín et al. 1996), so only the fundamental points will be briefly described here.

In this approach, the MQDO wave function is expressed as the product of a radial wave function and an angular wave function. The MQDO radial wave function is the analytical solution of a one-electron Schrödinger equation containing a parametric potential of the form:

$$V(r) = \frac{\lambda(\lambda + 1) - l(l + 1)}{2r^2} - \frac{1}{r}, \quad (4)$$

where  $l$  is the orbital angular momentum quantum number,  $\lambda$  is a parameter which determines the screening in the model potential, and  $r$  is the distance between the nucleus and the electron. The MQDO angular wave function is expressed as a symmetry-adapted linear combination of spherical harmonics, in a way that ensures that the molecular orbitals form basis for the different irreducible representations of the molecular point group. This allows to formulate separately the radial and angular contributions to the transition moment, both as closed-form analytical expressions.

The electronic transition moment for a transition between two unperturbed electronic states  $i$  and  $j$ , is expressed as

$$R_e = R_{ij}(r)M_{ij}, \quad (5)$$

where  $R_{ij}(r)$  is the radial contribution to the transition moment.  $M_{ij}$  is the angular contribution resulting from the integration of the angular functions of the  $i$  and  $j$  states involved in the transition, and that of the transition operator.

For diatomic molecules, the rovibronic line absorption oscillator strength is given by (Larsson 1983)

$$f_{v'J',v''J''} = \frac{8\pi^2 m c a_0^2}{3h} \nu_{v'J',v''J''} \frac{S_{J'J''}}{2J'' + 1}, \quad (6)$$

where  $\nu_{v'J',v''J''}$  is the frequency (in  $\text{cm}^{-1}$ ) of the rotational line and  $S_{J'J''}$  is the line strength (in atomic units).

If the Born–Oppenheimer approximation (Born & Oppenheimer 1927) is taken into account, the total wave function is separated into electronic and nuclear terms, and the latter can be approximated by the product of rotational and vibrational wave functions. Then, the line strength can be express as

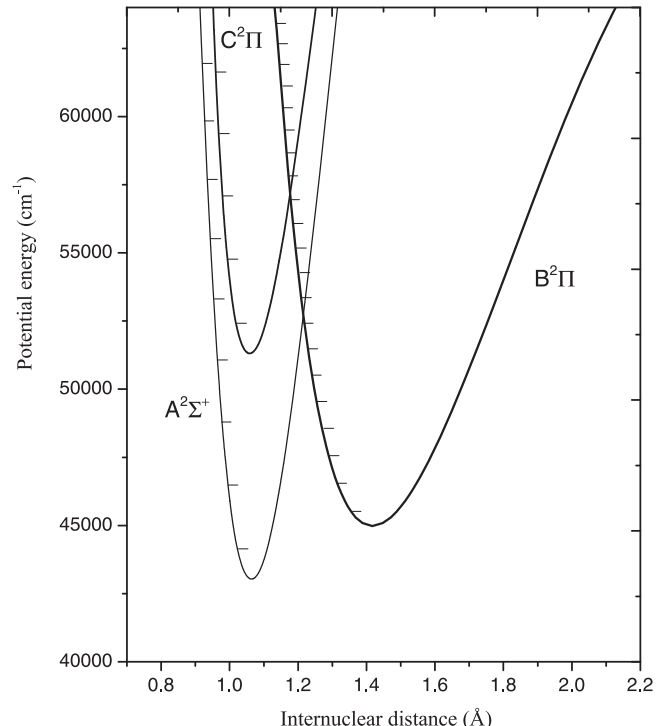


**Figure 1.** Diabatic potential energy curves for the  $C^2\Pi$ ,  $B^2\Pi$  and  $A^2\Sigma^+$  states of NO.

follows (Whiting & Nicholls 1974):

$$S_{J'J''} = q_{v'v''} R_e^2 \mathcal{J}_{J'J''}, \quad (7)$$

where  $q_{v'v''}$  is the Franck–Condon factor (FFC),  $\mathcal{J}_{J'J''}$  is the Hönl–London factor, and  $R_e$  is the electronic transition moment (in atomic units), which is presently calculated with the MQDO formalism. The FFC is given by the square of the overlap integral of the vibrational wave functions of the two states involved in the transition. In this work, the Rydberg–Klein–Rees (RKR; Rydberg 1931, Klein 1932, Rees 1947) approach is used to generate the potential energy curves of the electronic states, from which, the vibrational wave functions are obtained by solving the Schrödinger equation with the Numerov algorithm.

## 3. Results and Discussion

The  $A^2\Sigma^+$  and  $C^2\Pi$  excited states of NO molecule have Rydberg character. The  $A^2\Sigma^+$ , the lowest excited doublet state, is the first member of the  $ns\sigma$  Rydberg series and its electronic configuration is  $(1\sigma)^2(2\sigma)^2(3\sigma)^2(4\sigma)^2(1\pi)^4(5\sigma)^2(3s\sigma)^1$ . The  $C^2\Pi$  state, with electronic configuration  $(1\sigma)^2(2\sigma)^2(3\sigma)^2(4\sigma)^2(1\pi)^4(5\sigma)^2(3p\pi)^1$ , is the first member of the  $np\pi$  Rydberg series and, as already mentioned, it is perturbed by the  $B^2\Pi$  valence state. The rotational levels of the Rydberg  $A^2\Sigma^+$  state are characterized by spin-splitting, while those of the  $C^2\Pi$  state are characterized by both spin-splitting and  $\Lambda$ -doubling.

The diabatic potential energy curves of the  $C^2\Pi$ ,  $A^2\Sigma^+$  and  $B^2\Pi$  states are shown in Figure 1. These have been generated from the RKR approach using the molecular constants given by Engleman & Rouse (1971) for the  $A^2\Sigma^+$  state and by Galluser & Dressler (1982) for the  $C^2\Pi$  and  $B^2\Pi$  states. As the potential curves show, the lower state of the  $C^2\Pi(0)-A^2\Sigma^+(0)$  Rydberg transition is unperturbed, whereas the  $C^2\Pi(0)$  Rydberg state

**Table 1**  
 $C^2\Pi$  and  $B^2\Pi$  Fractions of the  $C^2\Pi_{1/2}$  and  $C^2\Pi_{3/2}$  Rotational Levels of NO

$J$	$C^2\Pi_{1/2}$		$C^2\Pi_{3/2}$	
	$C^2\Pi$	$B^2\Pi$	$C^2\Pi$	$B^2\Pi$
1.5	0.909	0.091	0.121	0.879
2.5	0.737	0.263	0.303	0.697
3.5	0.301	0.699	0.786	0.214
4.5	0.356	0.645	0.951	0.049
5.5	0.804	0.196	0.982	0.018
6.5	0.952	0.048	0.991	0.009
7.5	0.982	0.018	0.995	0.005
8.5	0.991	0.009	0.997	0.003

interacts with the  $B^2\Pi(7)$  valence state according to earlier studies on perturbations of excited states of the NO molecule (Lagerqvist & Miecher 1958; Amiot & Verges 1982). In a previous work (Lavín & Velasco 2022), we used the method of matrix diagonalization to treat the homogeneous interaction between the two doublet components of the  $C^2\Pi(0)$  Rydberg state  $C^2\Pi_{1/2}(0)$ ,  $C^2\Pi_{3/2}(0)$ , and the two doublet components of the valence  $B^2\Pi(7)$  state  $B^2\Pi_{1/2}(7)$ ,  $B^2\Pi_{3/2}(7)$ . Only a brief description of the procedure will be given here. The eigenvalues and eigenvectors for the four interacting states were obtained by diagonalization of a  $4 \times 4$  interaction matrix for each  $\Lambda$  doubling component and value of  $J$ . The diagonal elements of the matrix are the rotational energies of the unperturbed states. In the calculation of the energies of the unperturbed states, we used spectroscopic parameters reported by Amiot & Verges (1982) for the  $C^2\Pi(0)$  state and those of Murray et al. (1994) for the  $B^2\Pi(7)$  state. The off-diagonal matrix elements are the coupling parameters of the  $B^2\Pi(7)$  and  $C^2\Pi(0)$  states. Using a value of  $3.5 \text{ cm}^{-1}$  for the coupling parameters, the mean absolute deviation between the calculated rovibrational term energies and those derived from high-resolution measurements for the  $C^2\Pi_{1/2}(0)$ ,  $C^2\Pi_{3/2}(0)$ ,  $B^2\Pi_{1/2}(7)$ ,  $B^2\Pi_{3/2}(7)$  states (Braun et al. 2000; Murray et al. 1994) was of  $0.08 \text{ cm}^{-1}$ .

The fractional weights of  $C^2\Pi$  and  $B^2\Pi$  character in the perturbed rovibronic state  $i$  ( $C^2\Pi_{1/2}$ ,  $C^2\Pi_{3/2}$ ) obtained from the eigenvectors of the basis states are given by

$$C^2 = s_{iC1}^2 + s_{iC2}^2, \quad (8)$$

$$B^2 = s_{iB1}^2 + s_{iB2}^2, \quad (9)$$

being  $s_{iC1}$ ,  $s_{iC2}$ ,  $s_{iB1}$  and  $s_{iB2}$ , respectively, the eigenvectors for the  $C^2\Pi_{1/2}$ ,  $C^2\Pi_{3/2}$ ,  $B^2\Pi_{1/2}$ , and  $B^2\Pi_{3/2}$  basis states in the state  $i$ . The  $C^2\Pi$  and  $B^2\Pi$  fractions in the  $C^2\Pi_{1/2}$  and  $C^2\Pi_{3/2}$  perturbed states are listed in Table 1. Our results showed that the  $C^2\Pi(0)$  Rydberg and  $B^2\Pi(7)$  valence states are highly mixed with each other for  $J \leq 5.5$  values. Indeed, the electronic character of the  $C^2\Pi_{1/2}(0)$  Rydberg state at  $J$ -values of 3.5 and 4.5 is predominantly  $B^2\Pi(7)$  valence state. A similar behavior was observed for  $J$ -values of 1.5 and 2.5 of the  $C^2\Pi_{3/2}(0)$  Rydberg state.

The expression given for the line strength (Equation (7)) is appropriated when the states involved in the transition are not perturbed. To adequately model the intensity distribution of the rovibronic transitions studied in this work, the perturbation experienced by the  $C^2\Pi_{1/2}$  and  $C^2\Pi_{3/2}$  rotational states needs to be considered. Thus, to obtain the oscillator strengths, we have

used the following expression for the line strength:

$$S_{J'J''} = [C \langle v'_C | v'' \rangle R_e^C (\mathcal{J}_{J'J''})^{1/2} + B \langle v'_B | v'' \rangle R_e^B (\mathcal{J}_{J'J''})^{1/2}]^2, \quad (10)$$

where  $\langle v'_C | v'' \rangle$  is the vibrational overlap integral between the  $C^2\Pi(0)$  and  $A^2\Sigma^+(0)$  states and  $\langle v'_B | v'' \rangle$  is the vibrational overlap integral between the  $B^2\Pi(7)$  and  $A^2\Sigma^+(0)$  states.  $R_e^C$  and  $R_e^B$  are the electronic transition moments of the unperturbed  $C^2\Pi$ - $A^2\Sigma^+$  and  $B^2\Pi$ - $A^2\Sigma^+$  transitions, respectively.  $C$  and  $B$  are the square root of the fractional weights of  $C^2\Pi$  and  $B^2\Pi$  character, respectively, in the perturbed  $C^2\Pi_{1/2}$  and  $C^2\Pi_{3/2}$  states.

The FFCs calculated from the RKR potential curves are 0.995 for the  $C^2\Pi(0)$ - $A^2\Sigma^+(0)$  transition and  $1.2 \times 10^{-5}$  for the  $B^2\Pi(7)$ - $A^2\Sigma^+(0)$  transition. Because of its smaller Franck-Condon, the  $B^2\Pi(7)$ - $A^2\Sigma^+(0)$  contribution to the rovibronic transition moment in Equation (10) is negligible. We have calculated the electronic transition moment for the  $C^2\Pi$ - $A^2\Sigma^+$  Rydberg transition with the MQDO method, for which the ionization energy of NO and the energies of  $A^2\Sigma^+$  and  $C^2\Pi$  Rydberg states are required. We have taken the ionization energy reported by Reiser et al. (1988) and the energies of the  $A^2\Sigma^+$  and  $C^2\Pi$  states reported by Brunger et al. (2000). The MQDO electronic transition moment is 3.63 au. For the calculation of the Hönl-London factors, we have used the general expressions reported by Kovács (1969) for a  $^2\Pi$ - $^2\Sigma^+$  transition with  $\Delta\Lambda = +1$ , in the intermediate coupling case between Hund's case (a) and (b). An additional factor of 2 was introduced in each formula to account for the doublet  $\Lambda$  components.

The  $C^2\Pi(0)$ - $A^2\Sigma^+(0)$  gives rise to six main branches,  $P_{11}$ ,  $P_{22}$ ,  $Q_{11}$ ,  $Q_{22}$ ,  $R_{11}$ ,  $R_{22}$ , and six satellites branches,  $P_{12}$ ,  $P_{21}$ ,  $Q_{12}$ ,  $Q_{21}$ ,  $R_{12}$ , and  $R_{21}$ . In the notation used here, the first of the subscripts represents one of the two spin-split states of  $C^2\Pi$  and the second number represents one of the two spin-split states of the  $A^2\Sigma^+$  state. The transition wavenumbers, obtained considering the  $C^2\Pi(0) \sim B^2\Pi(7)$  interaction, for the rotational lines of the  $C^2\Pi_{1/2}(0)$ - $A^2\Sigma^+(0)$  and  $C^2\Pi_{3/2}(0)$ - $A^2\Sigma^+(0)$  Rydberg transitions are listed in Tables 2–4. We determine the line positions by subtracting the appropriate  $A^2\Sigma^+$  state term from each perturbed rovibronic term of the  $C^2\Pi$  state. Term values for the  $A^2\Sigma^+$  state were taken from Braun et al. (2000). The experimental transition wavenumbers reported by Amiot & Verges (1982) are included in Tables 2–4 for comparative purposes. Recently, Qu et al. (2021) determined rovibronic energy levels for excited electronic states of NO using the Measured Active Rotational-Vibrational Energy Levels (MARVEL) technique, as part of ExoMol project. We have also included the line positions derived from experimental MARVEL  $C^2\Pi(0)$  and  $A^2\Sigma^+(0)$  energy levels in the tables. As can be seen, a general good agreement between all data is found. The present line positions show a mean absolute deviation of  $0.08 \text{ cm}^{-1}$  from the most recent experimental data (Qu et al. 2021).

The absorption oscillator strengths for the rotational lines of the  $C^2\Pi(0)$ - $A^2\Sigma^+(0)$  band are also presented in Tables 2–4. When the  $C^2\Pi(0) \sim B^2\Pi(7)$  interaction is negligible, i.e., transitions that involve  $C^2\Pi(0)$  rotational states with  $J > 5.5$ , our results show a normal pattern of rovibronic intensities. The  $Q_{11}$  and  $Q_{22}$  branches are strong and of comparable intensity and the  $P_{11}$ ,  $P_{22}$ ,  $R_{11}$ , and  $R_{22}$  branches have about half the

**Table 2**  
Wavenumbers (in  $\text{cm}^{-1}$ ) and Line Oscillator Strengths for  $P$  Branches of the  $C^2\Pi(0)-A^2\Sigma^+(0)$  Band of NO

$J''$	$P_{11}$				$P_{12}$				$P_{22}$				$P_{21}$			
	$\nu^{\text{a}}$	$\nu^{\text{b}}$	$\nu^{\text{c}}$	$f\text{-value}^{\text{a}}$												
2.5	8169.070	8169.286	8169.340	7.14E-02	8157.055	8157.268	8157.325	3.30E-03	8169.335	8169.439	8169.433	1.01E-02	8181.270	8181.369	8181.364	1.04E-03
3.5	8168.155	8168.128	8168.113	7.41E-02	8152.115	8152.083	8152.074	1.43E-03	8159.895	8160.089	8160.111	3.12E-02	8175.845	8176.034	8176.051	1.35E-03
4.5	8163.767	8163.590	8163.547	3.41E-02	8143.834	8143.650	8143.613	3.74E-04	8152.044	8152.308	8152.356	9.02E-02	8172.177	8172.420	8172.456	2.11E-03
5.5	8155.599	8155.401	8155.415	4.33E-02	8131.813	8131.623	8131.638	3.02E-04	8146.933	8147.113	8147.146	1.17E-01	8171.239	8171.412		1.71E-03
6.5	8148.290	8148.160	8148.204	1.03E-01	8120.831	8120.714		4.76E-04	8142.531	8142.655	8142.677	1.26E-01	8171.020	8171.137		1.27E-03
7.5	8143.222	8143.184	8143.196	1.26E-01	8112.052	8112.019		4.19E-04	8138.292	8138.387	8138.400	1.31E-01	8170.982	8171.072		9.70E-04
8.5	8138.794	8138.781	8138.779	1.33E-01	8103.884	8103.884		3.38E-04	8134.104	8134.181	8134.188	1.35E-01	8171.034	8171.098		7.63E-04
9.5	8134.509	8134.522	8134.512	1.37E-01	8095.890	8095.916		2.74E-04	8129.940	8129.999	8130.002	1.38E-01	8171.119	8171.178		6.15E-04
10.5	8130.298	8130.312	8130.297	1.39E-01	8088.001	8088.028		2.26E-04	8125.781	8125.824	8125.823	1.40E-01	8171.248	8171.294		5.06E-04
11.5	8126.102	8126.120	8126.102	1.42E-01	8080.148	8080.189		1.89E-04	8121.608	8121.647	8121.645	1.42E-01	8171.412	8171.440		4.23E-04
12.5	8121.912	8121.933	8121.913	1.43E-01	8072.344	8072.389		1.61E-04	8117.434	8117.466	8117.461	1.43E-01	8171.582	8171.609		3.59E-04
13.5	8117.720	8117.743	8117.721	1.45E-01	8064.589	8064.619		1.38E-04	8113.249	8113.275	8113.268	1.45E-01	8171.780	8171.799		3.09E-04
14.5	8113.528	8113.547	8113.524	1.46E-01	8056.846	8056.877		1.20E-04	8109.056	8109.074	8109.851	1.46E-01	8171.998	8172.010		2.68E-04
15.5	8109.328	8109.344	8109.320	1.47E-01	8049.127	8049.161		1.05E-04	8104.847	8104.862	8104.851	1.47E-01	8172.238	8172.239		2.35E-04
16.5	8105.131	8105.130	8105.106	1.48E-01	8041.444	8041.469		9.3E-05	8100.634	8100.638	8100.626	1.48E-01	8172.501	8172.485		2.08E-04
17.5	8100.901	8100.906	8100.882	1.48E-01	8033.779	8033.800		8.3E-05	8096.409	8096.402	8096.389	1.48E-01	8172.771	8172.748		1.85E-04
18.5	8096.678	8096.670	8096.646	1.49E-01	8026.144	8026.153		7.4E-05	8092.154	8092.152	8092.139	1.49E-01	8173.058	8173.027		1.66E-04
19.5	8092.437	8092.422	8092.398	1.50E-01	8018.523	8018.529		6.7E-05	8087.903	8087.889	8087.876	1.50E-01	8173.357	8173.323		1.50E-04
20.5	8088.178	8088.162	8088.137	1.50E-01	8010.928	8010.926		6.0E-05	8083.638	8083.613	8083.598	1.50E-01	8173.678	8173.633		1.36E-04
21.5	8083.906	8083.888	8083.863	1.50E-01	8003.352	8003.344		5.5E-05	8079.352	8079.322	8079.308	1.50E-01	8174.016	8173.958		1.23E-04
22.5	8079.632	8079.601	8079.576	1.51E-01	7995.807	7995.783		5.0E-05	8075.057	8075.016	8075.002	1.51E-01	8174.372	8174.296		1.13E-04
23.5	8075.340	8075.299	8075.274	1.51E-01	7988.267	7988.243		4.6E-05	8070.747	8070.695	8070.681	1.51E-01	8174.730	8174.646		1.04E-04
24.5	8071.043	8070.982	8070.957	1.52E-01	7980.766	7980.721		4.2E-05	8066.426	8066.358	8066.343	1.52E-01	8175.123	8175.008		9.5E-05
25.5	8066.724	8066.649	8066.624	1.52E-01	7973.276	7973.217		3.9E-05	8062.096	8062.001	8061.986	1.52E-01	8175.524	8175.378		8.8E-05
26.5	8062.387	8062.297	8062.271	1.52E-01	7965.821	7965.729		3.6E-05	8057.751	8057.621	8057.606	1.52E-01	8175.927	8175.750		8.2E-05

**Notes.**<sup>a</sup> This work.<sup>b</sup> Qu et al. (2021).<sup>c</sup> Amiot & Verges (1982).

**Table 3**  
Wavenumbers (in  $\text{cm}^{-1}$ ) and Line Oscillator Strengths for R Branches of the  $C^2\Pi(0)-A^2\Sigma^+(0)$  Band of NO

$J''$	$R_{11}$				$R_{12}$				$R_{22}$				$R_{21}$			
	$\nu^a$	$\nu^b$	$\nu^c$	f-value <sup>a</sup>	$\nu^a$	$\nu^b$	$\nu^c$	f-value <sup>a</sup>	$\nu^a$	$\nu^b$	$\nu^c$	f-value <sup>a</sup>	$\nu^a$	$\nu^b$	$\nu^c$	f-value <sup>a</sup>
1.5	8188.014	8187.987		2.13E-01	8179.924	8179.891	8179.885	9.06E-03	8187.704	8187.898	8187.918	8.55E-02	8195.704	8195.893	8195.920	1.68E-03
2.5	8191.570	8191.393	8191.359	7.43E-02	8179.585	8179.400	8179.367	1.80E-03	8187.795	8188.059	8188.111	1.92E-01	8199.980	8200.223	8200.281	2.03E-03
3.5	8191.345	8191.147	8191.164	8.03E-02	8175.505	8175.315	8175.350	1.24E-03	8190.625	8190.805	8190.840	2.13E-01	8206.985	8207.158		1.41E-03
4.5	8191.977	8191.847	8191.892	1.71E-01	8172.464	8172.346	8172.375	1.76E-03	8194.164	8194.288	8194.310	2.08E-01	8214.707	8214.824		9.53E-04
5.5	8194.849	8194.812	8194.825	1.95E-01	8171.623	8171.590	8171.589	1.44E-03	8197.863	8197.958	8197.971	2.03E-01	8222.609	8222.699		6.78E-04
6.5	8198.360	8198.348	8198.345	1.96E-01	8171.391	8171.391		1.10E-03	8201.611	8201.688	8201.696	1.98E-01	8230.600	8230.664		5.06E-04
7.5	8202.012	8202.025	8202.014	1.93E-01	8171.332	8171.357		8.54E-04	8205.382	8205.441	8205.444	1.94E-01	8238.622	8238.681		3.91E-04
8.5	8205.734	8205.749	8205.733	1.91E-01	8171.374	8171.400		6.81E-04	8209.154	8209.197	8209.196	1.91E-01	8246.684	8246.730		3.12E-04
9.5	8209.469	8209.488	8209.470	1.88E-01	8171.450	8171.490		5.55E-04	8212.910	8212.949	8212.946	1.88E-01	8254.779	8254.807		2.54E-04
10.5	8213.208	8213.229	8213.208	1.86E-01	8171.571	8171.615		4.61E-04	8216.661	8216.693	8216.687	1.86E-01	8262.878	8262.905		2.11E-04
11.5	8216.942	8216.965	8216.943	1.85E-01	8171.738	8171.767		3.89E-04	8220.398	8220.424	8220.417	1.85E-01	8271.002	8271.021		1.78E-04
12.5	8220.672	8220.691	8220.669	1.83E-01	8171.914	8171.944		3.33E-04	8224.124	8224.142	8224.133	1.83E-01	8279.142	8279.154		1.53E-04
13.5	8224.390	8224.406	8224.382	1.82E-01	8172.109	8172.142		2.88E-04	8227.829	8227.844	8227.834	1.82E-01	8287.300	8287.301		1.32E-04
14.5	8228.108	8228.107	8228.083	1.81E-01	8172.336	8172.360		2.51E-04	8231.526	8231.530	8231.519	1.81E-01	8295.478	8295.462		1.15E-04
15.5	8231.788	8231.793	8231.769	1.80E-01	8172.577	8172.597		2.21E-04	8235.207	8235.200	8235.187	1.80E-01	8303.658	8303.635		1.02E-04
16.5	8235.471	8235.463	8235.438	1.79E-01	8172.844	8172.851		1.96E-04	8238.854	8238.852	8238.838	1.79E-01	8311.851	8311.820		9.0E-05
17.5	8239.131	8239.116	8239.092	1.78E-01	8173.119	8173.123		1.75E-04	8242.499	8242.485	8242.471	1.78E-01	8320.051	8320.017		8.1E-05
18.5	8242.768	8242.752	8242.727	1.78E-01	8173.414	8173.411		1.58E-04	8246.124	8246.099	8246.086	1.78E-01	8328.268	8328.223		7.3E-05
19.5	8246.387	8246.369	8246.344	1.77E-01	8173.723	8173.714		1.42E-04	8249.723	8249.693	8249.679	1.77E-01	8336.497	8336.439		6.6E-05
20.5	8249.998	8249.967	8249.942	1.77E-01	8174.058	8174.033		1.29E-04	8253.308	8253.267	8253.252	1.77E-01	8344.738	8344.662		6.0E-05
21.5	8253.586	8253.544	8253.520	1.76E-01	8174.392	8174.365		1.18E-04	8256.872	8256.820	8256.805	1.76E-01	8352.976	8352.892		5.5E-05
22.5	8257.162	8257.101	8257.076	1.76E-01	8174.757	8174.711		1.08E-04	8260.417	8260.349	8260.334	1.76E-01	8361.242	8361.127		5.0E-05
23.5	8260.710	8260.634	8260.610	1.75E-01	8175.127	8175.067		9.9E-05	8263.947	8263.852	8263.836	1.75E-01	8369.510	8369.364		4.6E-05
24.5	8264.233	8264.143	8264.117	1.75E-01	8175.526	8175.433		9.2E-05	8267.456	8267.326	8267.310	1.75E-01	8377.773	8377.596		4.3E-05
25.5	8267.744	8267.621	8267.596	1.75E-01	8175.936	8175.801		8.5E-05	8270.926	8270.760	8270.743	1.75E-01	8386.054	8385.813		3.9E-05

**Notes.**<sup>a</sup> This work.<sup>b</sup> Qu et al. (2021).<sup>c</sup> Amiot & Verges (1982).

**Table 4**  
Wavenumbers (in  $\text{cm}^{-1}$ ) and Line Oscillator Strengths for  $Q$  Branches of the  $C^2\Pi(0)-A^2\Sigma^+(0)$  Band of NO

$J''$	$Q_{11}$				$Q_{12}$				$Q_{22}$				$Q_{21}$			
	$\nu^a$	$\nu^b$	$\nu^c$	f-value <sup>a</sup>	$\nu^a$	$\nu^b$	$\nu^c$	f-value <sup>a</sup>	$\nu^a$	$\nu^b$	$\nu^c$	f-value <sup>a</sup>	$\nu^a$	$\nu^b$	$\nu^c$	f-value <sup>a</sup>
1.5	8176.924	8177.135	8177.190	2.73E-01	8169.064	8169.281	8169.340	6.7E-05	8181.264	8181.363	8181.364	3.73E-02	8189.204	8189.308	8189.301	6.01E-04
2.5	8179.930	8179.896	8179.885	2.36E-01	8168.145	8168.120	8168.113	5.9E-06	8175.835	8176.024	8176.051	9.91E-02	8187.710	8187.904	8187.918	3.92E-04
3.5	8179.595	8179.408	8179.367	1.02E-01	8163.755	8163.580	8163.547	7.9E-06	8172.165	8172.408	8172.456	2.57E-01	8187.805	8188.069	8188.110	4.32E-04
4.5	8175.517	8175.324	8175.350	1.22E-01	8155.584	8155.390	8155.415	1.1E-05	8171.224	8171.397	8171.437	3.08E-01	8190.637	8190.817	8190.840	2.80E-04
5.5	8172.479	8172.357	8172.403	2.66E-01	8148.273	8148.146	8148.204	2.3E-05	8171.003	8171.120	8171.158	3.19E-01	8194.179	8194.303		1.77E-04
6.5	8171.640	8171.603	8171.618	3.10E-01	8143.201	8143.169		2.5E-05	8170.961	8171.051	8171.085	3.22E-01	8197.880	8197.975		1.20E-04
7.5	8171.412	8171.407	8171.409	3.20E-01	8138.772	8138.764		2.2E-05	8171.012	8171.076	8171.085	3.24E-01	8201.632	8201.709		8.6E-05
8.5	8171.354	8171.375	8171.365	3.23E-01	8134.484	8134.503		2.0E-05	8171.094	8171.153	8171.158	3.25E-01	8205.404	8205.463		6.4E-05
9.5	8171.399	8171.420	8171.408	3.24E-01	8130.270	8130.290		1.7E-05	8171.220	8171.266	8171.279	3.25E-01	8209.179	8209.222		5.0E-05
10.5	8171.478	8171.512	8171.494	3.25E-01	8126.071	8126.096		1.5E-05	8171.381	8171.409	8171.408	3.25E-01	8212.938	8212.977		3.9E-05
11.5	8171.602	8171.639	8171.618	3.25E-01	8121.878	8121.907		1.3E-05	8171.548	8171.575	8171.589	3.26E-01	8216.692	8216.724		3.2E-05
12.5	8171.772	8171.793	8171.772	3.26E-01	8117.684	8117.715		1.2E-05	8171.744	8171.763	8171.772	3.26E-01	8220.432	8220.458		2.7E-05
13.5	8171.950	8171.972	8171.953	3.26E-01	8113.489	8113.517		1.1E-05	8171.959	8171.971	8171.976	3.26E-01	8224.160	8224.178		2.2E-05
14.5	8172.148	8172.172	8172.151	3.26E-01	8109.286	8109.312		9.5E-06	8172.196	8172.197	8172.205	3.26E-01	8227.868	8227.883		1.9E-05
15.5	8172.378	8172.392	8172.371	3.26E-01	8105.087	8105.096		8.5E-06	8172.457	8172.441	8172.453	3.26E-01	8231.568	8231.572		1.7E-05
16.5	8172.621	8172.631	8172.609	3.26E-01	8100.854	8100.870		7.7E-06	8172.724	8172.701	8172.711	3.26E-01	8235.251	8235.244		1.4E-05
17.5	8172.891	8172.888	8172.866	3.26E-01	8096.629	8096.632		7.0E-06	8173.009	8172.978	8172.988	3.26E-01	8238.901	8238.899		1.3E-05
18.5	8173.168	8173.162	8173.139	3.26E-01	8092.384	8092.382		6.4E-06	8173.304	8173.270	8173.281	3.26E-01	8242.548	8242.534		1.1E-05
19.5	8173.467	8173.451	8173.429	3.26E-01	8088.123	8088.119		5.9E-06	8173.623	8173.578	8173.589	3.26E-01	8246.177	8246.152		1.0E-05
20.5	8173.778	8173.757	8173.735	3.26E-01	8083.848	8083.843		5.4E-06	8173.958	8173.900	8173.911	3.26E-01	8249.778	8249.748		9.0E-06
21.5	8174.116	8174.078	8174.056	3.26E-01	8079.572	8079.554		5.0E-06	8174.312	8174.236	8174.247	3.27E-01	8253.366	8253.325		8.1E-06
22.5	8174.452	8174.412	8174.390	3.26E-01	8075.277	8075.250		4.6E-06	8174.667	8174.583	8174.596	3.27E-01	8256.932	8256.880		7.4E-06
23.5	8174.820	8174.760	8174.737	3.27E-01	8070.977	8070.931		4.3E-06	8175.057	8174.942	8174.954	3.27E-01	8260.480	8260.412		6.7E-06
24.5	8175.193	8175.118	8175.096	3.27E-01	8066.656	8066.596		4.0E-06	8175.456	8175.310	8175.325	3.27E-01	8264.013	8263.918		6.1E-06
25.5	8175.594	8175.486	8175.462	3.27E-01	8062.316	8062.242		3.7E-06	8175.856	8175.679	8175.690	3.27E-01	8267.524	8267.394		5.6E-06
26.5	8176.007	8175.856	8175.831	3.27E-01	8057.971	8057.865		3.5E-06	8176.281	8176.040	8176.048	3.27E-01	8270.997	8270.831		5.2E-06

**Notes.**<sup>a</sup> This work.<sup>b</sup> Qu et al. (2021).<sup>c</sup> Amiot & Verges (1982).

intensity of the  $Q_{11}$  and  $Q_{22}$  branches. The intensity of the satellites branches is small compared to that of the main branches. However, at low  $J$ -values, our calculations indicate that the lines of all branches are weaker than predicted by Hönl–London factors, as consequence of the perturbing effect of the  $B^2\Pi(7)$  valence state. So,  $f$ -values for transitions ending in the  $C^2\Pi_{1/2}(0)$  with  $J$ -values of 3.5 and 4.5, and  $C^2\Pi_{3/2}(0)$  with  $J = 2.5$  rotational states, which are predominantly  $B^2\Pi$  states, are about 3 times lower than expected on the basis of Hönl–London factors. For transitions ending in the  $J = 1.5$  level of the  $C^2\Pi_{3/2}(0)$  state, the decrease in the line oscillator strengths is more noticeable, about 10 times lower than nonperturbed  $f$ -values, due to the high percentage (88%) of  $B^2\Pi(7)$  valence character of this Rydberg state.

No comparative data, as far as we know, have been reported in the literature for oscillator strengths of the rotational lines belonging to the  $C^2\Pi(0)$ - $A^2\Sigma^+(0)$  band. We have calculated the band oscillator strength for which an experimental result (Groth et al. 1971) has been found in the literature. To determine the oscillator strength for such band, first we calculate the integrated absorption cross sections for the individual rotational lines of the  $C^2\Pi(0)$ - $A^2\Sigma^+(0)$  band through the expression given by Nicholls (1969):

$$\int_{J'J''} \sigma(\nu) d\nu = \frac{\pi e^2}{mc^2} \frac{N_{J''}}{N_{tot}} f_{v'v''}, \quad (11)$$

where  $\nu$  is the frequency in  $\text{cm}^{-1}$  and  $N_{J''}/N_{tot}$  is the relative population of the rotational level  $J''$  of the lower electronic state. We assumed a Boltzmann distribution for the rotational populations, which were obtained at a temperature of 295 K. Then, we derive the band  $f$ -value,  $f_{v'v''}$ , by adding up the integrated absorption cross-section contributions from all the rotational lines and, finally, the resulting value is converted into band oscillator strength by using the equation (Morton & Noreau 1994):

$$f_{v'v''} = \frac{mc^2}{\pi e^2} \int \sigma(\nu) d\nu. \quad (12)$$

The thus calculated oscillator strength for the  $C^2\Pi(0)$ - $A^2\Sigma^+(0)$  band is 0.57, which conforms well with the value of 0.61 derived by Groth et al. (1971) using the ratio of the measured intensities of the  $\gamma$ - and  $\delta$ -band systems. Note that the band  $f$ -value reported by Groth et al. (1971) was determined from indirect measurements on the  $C^2\Pi$  Rydberg state, while our result is obtained from direct calculations of the lines  $f$ -values of the  $C^2\Pi(0)$ - $A^2\Sigma^+(0)$ .

Summarizing, in this study, we present transition energies and oscillator strengths for the rotational lines of the  $C^2\Pi(0)$ - $A^2\Sigma^+(0)$  band in nitric oxide. Our results show that the interaction between the  $C^2\Pi(0)$  Rydberg and  $B^2\Pi(7)$  valence states at low  $J$ -values lead to significant deviations from predictions based on Hönl–London factors. It is thus evident that the line oscillator strengths cannot be reliably deduced from the band oscillator strength. As far as we know,  $f$ -values for the  $C^2\Pi(0)$ - $A^2\Sigma^+(0)$  band at the rotational level are

reported here for the first time. The data presented in this work provide useful information to interpret the Venus Express VIRTIS observations in the nightglow upper atmosphere of Venus where this band has been detected.

## Acknowledgments

This work has been supported by the Junta de Castilla y León (UCI 139, grant VA244P20).

## ORCID iDs

A. M. Velasco <https://orcid.org/0000-0003-3835-6873>

## References

- Ackerman, F., & Miescher, E. 1969, *JMoSp*, **31**, 400  
 Amiot, C., & Verges, J. 1982, *PhyS*, **25**, 302  
 Barth, C. A. 1964, *JGR*, **69**, 3301  
 Benesch, W. M., & Saum, K. A. 1972, *JQSRT*, **12**, 1129  
 Bertaux, J.-L., Leblanc, G., Severine, P., et al. 2005, *Sci*, **307**, 566  
 Born, M., & Oppenheimer, R. 1927, *AnP*, 389, 20  
 Braun, V. D., Huber, K. P., Vervloet, M., et al. 2000, *JMoSp*, **203**, 65  
 Brunger, M. J., Campbell, L., Cartwright, D. C., et al. 2000, *JPhB*, **33**, 783  
 Cohen-Sabban, J., & Vuillemin, A. 1973, *Ap&SS*, **24**, 127  
 Dingle, T. W., Freedman, P. A., Gelernt, B., Jones, W. J., & Smith, I. W. M. 1975, *CP*, **8**, 171  
 Engleman, R., & Rouse, P. E. 1971, *JMoSp*, **37**, 240  
 Feldman, P. D., Moos, H. W., Clarke, J. T., & Lane, A. L. 1979, *Natur*, **279**, 221  
 Feldman, P. D., & Takacs, P. Z. 1974, *GeoRL*, **1**, 169  
 Galluser, R., & Dressler, K. 1982, *JChPh*, **76**, 4311  
 Gerin, M., Viala, Y., Pauzat, F., & Ellinger, Y. 1992, *A&A*, **266**, 463  
 Groth, W., Kley, D., & Schurath, U. 1971, *JQSRT*, **11**, 1475  
 Klein, O. 1932, *ZPhy*, **76**, 226  
 Kovács, I. 1969, *Rotational Structure of Diatomic Molecules* (New York: Elsevier)  
 Lagerqvist, A., & Miecher, E. 1958, *AcHPh*, **31**, 221  
 Larsson, M. 1983, *A&A*, **128**, 291  
 Lavín, C., & Velasco, A. M. 2022, *ApJ*, **941**, 29  
 Lin, M. C. 1974, *IJQE*, **10**, 516  
 Liszt, H. S., & Turner, B. E. 1978, *ApJL*, **224**, L73  
 Martín, I., Lavín, C., Velasco, A. M., et al. 1996, *CP*, **202**, 307  
 Martin, S., Mauersberger, R., Martin-Pintado, J., García-Burillo, S., & Henkel, C. 2003, *A&A*, **411**, L465  
 McGonagle, D., Ziurys, L. M., Irvine, W. M., & Minh, Y. C. 1990, *ApJ*, **359**, 121  
 Morton, D. C., & Noreau, L. 1994, *ApJS*, **95**, 301  
 Muñoz, A. G., Mills, F. P., Piccioni, G., & Drossart, P. 2009, *PNAS*, **106**, 985  
 Murray, J. E., Yoshino, K., Esmond, J. R., et al. 1994, *JChPh*, **101**, 62  
 Nicholls, R. W. 1969, *Electronic Spectra of Diatomic Molecules* (New York: Elsevier)  
 Qu, Q., Yurchenko, S. N., & Tennyson, J. 2021, *MNRAS*, **504**, 5768  
 Quintana-Lacaci, G., Agúndez, M., Cernicharo, J., et al. 2013, *A&A*, **560**, L2  
 Rees, A. L. G. 1947, *PPSL*, **59**, 998  
 Nicholls, R. W. 1969, *Electronic Spectra of Diatomic Molecules* (New York: Elsevier)  
 Reiser, G., Habenicht, W., Muller-Dethlefs, K., & Schlag, E. W. 1988, *CPL*, **152**, 119  
 Rydberg, R. 1931, *ZPhy*, **73**, 376  
 Stewart, A. I., & Barth, C. A. 1979, *Sci*, **205**, 59  
 Tennyson, P. D., Feldman, P. D., Hartig, G. F., & Henry, R. C. 1986, *JGR*, **91**, 10141  
 Velasco, A. M., Lavín, C., Bustos, E., et al. 2010, *JPCA*, **114**, 8450  
 Whiting, R. E., & Nicholls, R. W. 1974, *ApJS*, **27**, 1  
 Wray, K. L. 1969, *JQSRT*, **9**, 255  
 Young, R. A., & Sharpless, R. L. 1962, *Discuss. Faraday Soc.*, **33**, 228  
 Ziurys, L. M., McGonagle, D., Minh, Y., & Irvine, W. M. 1991, *ApJ*, **373**, 535